Dielectric Hysteresis of Heterogeneous Water Distribution observed in Soil's Wetting and Drying Process by GPR

A. Janet F. C. Sham, B. Wallace, W. L. Lai , C. H.C. Leung

Department of Land Surveying and Geo-Informatics, Faculty of Construction and Environment,

The Hong Kong Polytechnic University, Hong Kong

A. Janet.sham@polyu.edu.hk, B. leunghongching@gmail.com, C. wllai@polyu.edu.hk

Abstract **- This paper studies the phenomenon of dielectric hysteresis due to different extents of heterogeneities of water distribution in soil on variation of GPR wave velocity/ dielectric constant in a very porous plant soil. Relatively homogeneous (RHWD) and relatively inhomogeneous water distributions (RIWD) in soil were studied and compared by varying the water content through a wetting and drying cycle in a tank (2.02m long x 1.75m wide x 1m deep) filled with 750mm thick plant soil. During the cycle, a 900MHz antenna was used to capture GPR radargrams on a buried steel pipe regularly. Hyperbolic reflections of a buried pipe at fixed position were extracted to measure wave velocities/dielectric constants at different RHWD and RIWD in the wetting and drying cycle. A vertical coaxial-based water content sensor was also installed in a vertical standpipe in the middle of the tank to obtain the vertical water content profile, synchronize with and correlate to the GPR wave velocity/dielectric constant of soil. The result of cross plot between dielectric constant and degree of water saturation shows that (1) radargram images were highly disturbed during RIWD but were relatively clear during RHWD in both dry and saturated conditions, and (2) velocity and dielectric hysteresis were observed during the wetting and drying cycle, indicating not only the absolute water content, but also the distribution of water, play an important role on the increase/decrease of GPR wave velocity and dielectric constant.**

Index Terms**- dielectric hysteresis, relatively homogeneous water distributions (RHWD), relatively heterogeneous water distribution (RIWD), GPR wave velocity, soil permittivity**

I. INTRODUCTION

The vadose zone and the aquifer underneath in soil regulates the natural water cycle and the dependent ecosystem of the nature. The vadose zone plays a critical role in transporting fresh ground water naturally replenished by irrigation, precipitation and also from streams and rivers etc. The ground water on the other hand discharged by plant absorption, evaporation and surface runoff. The rate of replenishment and discharges within the vadose zone is depending on the textures, soil types, compaction, pore size distribution, pores shapes and clay contents of soil. There are studies concerning hydraulic conductivity [1] and capillary fringe [2]. These studies enhances our knowledge of hydrological parameters of the vadose zone and the aquifer.

Estimation of hydrological parameters is traditionally conducted by localized measurements which are limited to standard aquifer and slug tests conducted within sparse boreholes. These methods are inadequate to provide satisfactory spatial data resolution. In order to compensate and optimize the spatial resolution of these parameters, inversion of hydrological data [3] some near-surface geophysical (NSG) methods [4] such as ground probing devices, borehole tomography and remote sensing can be applied.

One of the promising NSG methods for investigation of hydrological data is GPR. In this study, GPR is selected to study the wetting and drying cycle in soil because of its high vertical resolution. It is a simulation of wetting and drying activities occurred in vadose zone. Besides, pump well test has been used with GPR for aquifer imaging

Water is one of the most influential factors affecting GPR's EM wave properties because of its dipolar molecular structure which couples with EM wave's polarization. Therefore, usually, GPR is applied to measure the depth of water table [5] and in recent years volumetric soil water content [6]. Quite often in common dielectric mixing models such as Complex refractive index model (CRIM) [7] and Topp's model [8], the wetting history or how heterogeneous water distributes in the soil is not taken in to account. This factor is studied in this paper. GPR was used to measure the different effects of RHWD and RIWD on the reflected radar signal of a buried pipe at 200mm deep. It was carried out by varying states of water in soil via RHWD/RIWD in a wetting/drying cycle, and analysis of wave velocity directly relating to dielectric constant. Pattern of dielectric hysteresis is observed in such wetting and drying processes, which simulates the water and dewater activities occurred in vadose zone.

II. BACKGROUND

A. Ground Penetrating Radar

GPR operates by emitting electromagnetic pulses into the subsurface and receiving the reflected pulses. When a signal is incident on a layer embedded in a medium such as water, signals are partially transmitted and reflected. Signals enter the layer bounce between the interfaces and re-emit reflected and transmitted signal replicas, which occur at fixed time delays or fixed phase shift [9].

Two-way travel time (TTT) of the EM wave of GPR is the time taken that the wave from the transmitter to the object which reflected the wave and back to the receiver. The travelling time is usually measure in nanosecond (ns) i.e. 1 x 10^{-9} s.

In general, we can calculate the velocity of the EM wave by the following equation (1)[10] when the depth of an object is known [10].

$$v = \frac{2D}{t} \qquad (1)$$

where "D" is the cover depth of the object (m) when the antenna is directly on top of the object, "v" is the velocity of the EM wave (m/ns) in the material and "t" is the two-way travel time (ns) of the GPR wave traveling in the material. . This relationship was further modified with an in-house developed GPR wave velocity algorithm [11]. In this algorithm, discrete velocities of each point of the reflected signals across the hyperbolic reflection of the object are measured.

B. Homogeneity and Heterogeneity

Homogeneity and heterogeneity are concepts that is relating to the uniformity in a substance or material. Soil is homogeneous because of its uniform in composition or character i.e. particle size, distribution, moisture content. In contrast, heterogeneous means non-uniform in the above qualities. In this experiment, water is added into the soil bulk to change the degree of heterogeneity of the soil bulk comprised of solid, water and air. RHWD means the touch-dry or completely saturated state of the soil; while RIWD means two intermediate states of wetted soil (1) from the touch-dry to completely saturated state (i.e. wetting process); and (2) from the completely saturated state to the state after the drying/pumping finished (i.e. drying process)

EM wave is scattered as it disputes the electric field of the wave propagation. It attenuates and scatters EM wave, affecting the GPR wave propagation by restricting the degree of polarization under the influence of an electric field. The relationship between the dielectric constant of a medium and the EM wave velocity propagates within it can be explained by the following equation (2).

$$v = \frac{c}{\sqrt{\varepsilon}} \qquad (2)$$

where c is the speed of light (0.3m/ns) and ε is dielectric constant.

III. AS A RESULT, ONCE THE VELOCITY IS ESTIMATED, THE DIELECTRIC CONSTANT OF THE MATERIAL CAN ALSO BE FOUND. THE ABOVE METHOD IS USED TO CALCULATE THE DIELECTRIC CONSTANT OF A MATERIAL BY RETRIEVING VELOCITY FROM RADAR SIGNAL. SUCH FORMULATION BECOMES MUCH COMPLICATED WHEN WATER OCCUPIES EVEN A SMALL VOLUME IN ANY POROUS NON-METALLIC MATERIAL. THE DIPOLE MOMENT OF WATER MANIFESTS ITSELF A UNIQUE DIELECTRIC AND POLARIZATION MECHANISM WHEN A HIGH-FREQUENCY EM WAVE ENTERS INTO THE MEDIA. AN INDIRECT METHOD TO MEASURE THE DIELECTRIC CONSTANT AT FREQUENCIES BETWEEN 10 MHZ AND 1 GHZ WITH THE VOLUMETRIC WATER CONTENT IS DETERMINED EMPIRICALLY IN THE LABORATORY CONDUCTED BY TOPP'S TEAM [8] AND DIFFERENT DIELECTRIC MIXING MODELS [7, 8, 12].EXPERIMENTAL SETUP

The experiment was carried out in the Underground Utility Survey Laboratory in the Hong Kong Polytechnic University. A soil tank with dimension 1.5m x 1.9m x 0.9m was constructed and a network of water pipes drilled with a number of evenly spaced holes were installed and overhung above the soil tank. It is used to simulate water precipitation into the soil (i.e. wetting). Besides, a pump well located at the upper left corner of the tank. The well is made of a perforated tube wrapped with geotextile. A sump pump was put in the well at the start of the drying cycle and pump water out of the soil tank. This setup of overhung water pipes and pump well simulates wetting and drying cycle in the soil under test (Figure 1).

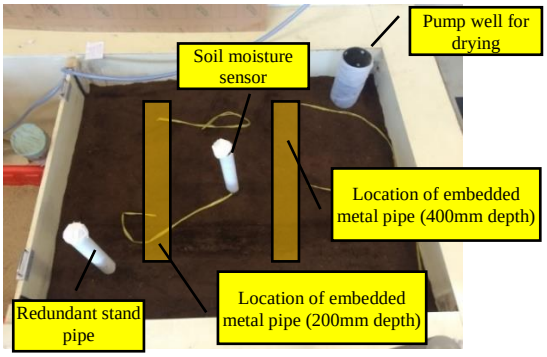

Figure 1 Tank for experiment

In addition, a calibrated coaxial-based water content sensor (Enviroscan, as shown in Figure 2) connected with a data

logger (data collection in every 60 seconds) was placed in the middle of the tank to measure variation of soil moisture data collection in the wetting and dry cycle. Lastly, two metal pipes with diameter 138mm were embedded inside the soil tank at 200mm and 400mm depths. It serves as a perfect target to be picked up by the 900MHz GPR for velocity estimation of the GPR wave in the soil. The soil used in the experiment was standard garden soil with very low density. The schematic diagram of the experimental setup is shown in Figure 3.

Figure 2: Photo of Enviroscan water content probe.

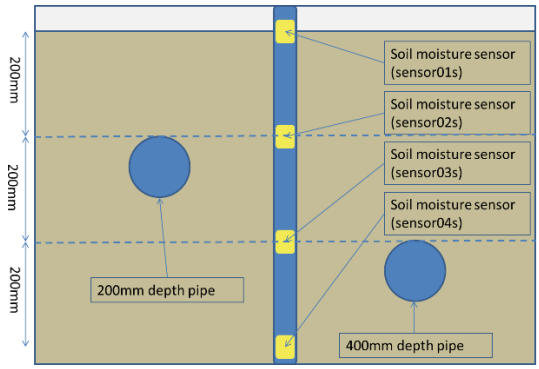

Figure 3 Schematic diagram of experimental setup (cross section)

IV. DATA COLLECTION

C. GPR data collection

A GSSI 900MHz GPR with SIR-20 control unit was used in this experiment for GPR data collection. A plastic plate with 100mm grid is made for GPR data collection. Data was collected by traversing the GPR antenna (900MHz) along the blue line shown in Figure 4.

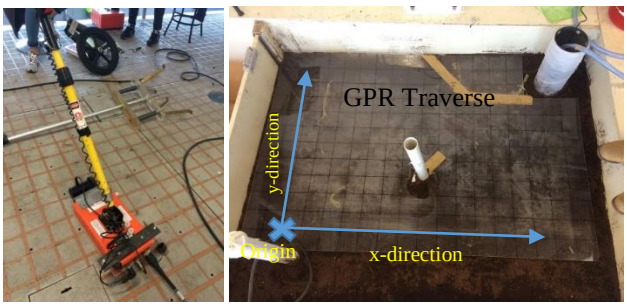

Figure 4 (a) Photo of 900MHz GPR and (b) Grid setting

A cycle of wetting and drying was conducted and 21 radargrams (as shown in Figure 5) were collected (12 wetting and 9 drying).

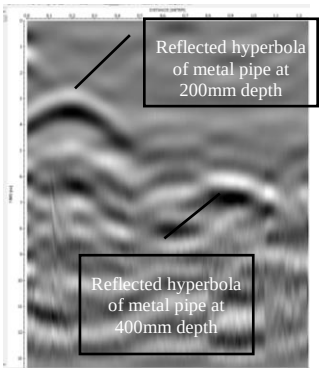

Figure 5 Processed radargram before wetting

The time for each data collection was chosen based on the significance of increase or decrease of soil moisture content revealed by distinct reading increments (during wetting) or decrements (during drying) recorded by the soil moisture sensors. For wetting, data was collected for each 3-4 units of increase in reading (2~7%) while for drying, data was collected for each 3-4 decrease in reading (~7%). The wetting process is shown in the following Figure 6. The maximum reading of volumetric soil water content calibrated in saturated soil was 47.7% while the minimum reading calibrated for touch-dry soil was 4.3%.

Figure 6 Wetting process

The whole wetting process (Figure 6) was considered to be completed once the soil was fully saturated i.e. both visually from the top and moisture sensor reading being constant. Similarly, the whole drying process was completed, when the drying rate of the soil becomes constant.

The GPR data was processed by several signal processing techniques: subtract DC-shift, dewow, gain adjustment, time-zero correction, bandpass butterworth and background removal (Figure 5). GPR antenna records the

whole waveform (A-scan) with amplitude at discrete time. The location of reflector is recognized by locating the time with stronger reflection (either positive or negative polarity). Travelling velocities of the GPR signal at different wetting and drying cycles were estimated by identifying the travelling time of the hyperbolic signals oblique and normal to the pipe, using an in-house developed algorithm and program [13]. The algorithm enables calculation of the wave velocity of discrete travelling time of signal reflected from the embedded object (Figure 7). The assumption of using the above modified equation is 1) the embedded object is round in shape, 2) data collection by common-offset survey method and 3) constant velocity within the covered region of the medium.

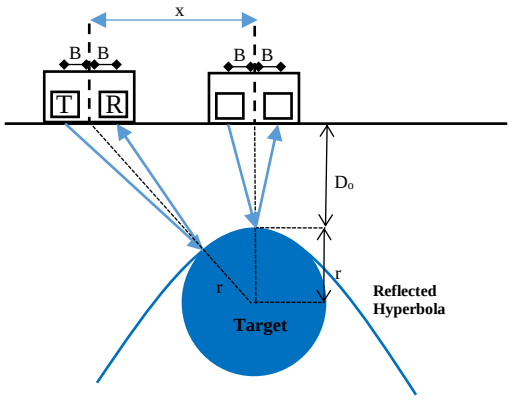

Figure 7 Schematic diagram of velocity estimation by analysis of GPR signal.

$$v(x) = \frac{\sqrt{\left[(D_o + r) - \frac{(D_o + r)r}{\sqrt{(D_o + r)^2 + x^2}}\right]^2 + \left[\left(x - \frac{r \times x}{\sqrt{(D_o + r)^2 + x^2}}\right) - B\right]^2} + \sqrt{\left[(D_o + r) - \frac{(D_o + r)r}{\sqrt{(D_o + r)^2 + x^2}}\right]^2 + \left[\left(x - \frac{r \times x}{\sqrt{(D_o + r)^2 + x^2}}\right) + B\right]^2}}{t_x} \quad \textbf{(3)}$$

The Equation (3) requires the input of 'D_o' as the depth of the object, radius of the object 'r', 'x' the horizontal distance of the antenna from any oblique relative to the normal position of the target; 't_x' the two way travel time of the reflection from the transmitting/receiving antennae to the target at any distance 'x' and also 'B', half of the antenna separation (Figure 7).

D. Soil moisture measured by vertical moisture sensors

In this study, the collected moisture contents were used to correlate with the GPR wave velocity reflected from the two embedded metal pipes. Hence, only data from Sensor02s and Sensor03s (the closest sensors to the two metal pipes) were chosen for investigation (Figure 3). The following graphs reflect the pattern for both wetting and drying the data collected from soil moisture sensors. Degree of saturation (i.e. 0 for over-dried soil, 1 for completely saturated soil) rather than moisture content are used for presenting the wetness of the soil because moisture content will be affected by several parameters such as the compactness of the soil, porosity of soil and type of soil.

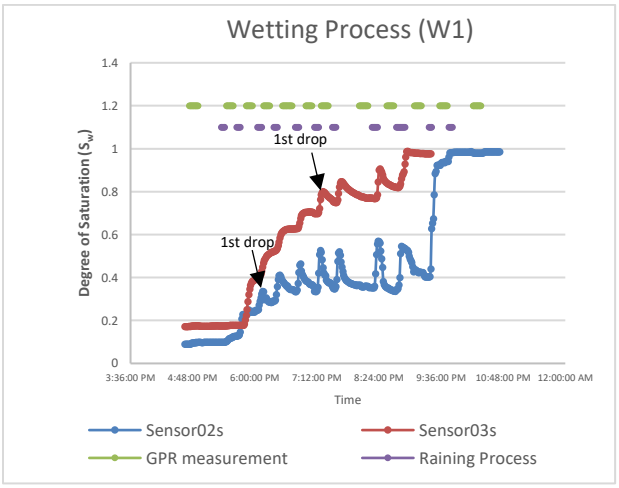

Figure 8 Degree of saturation (S_w) during wetting process

As shown in

Figure 8, both two sensors 02s and 03s experienced a subtle decrease in the degree of saturation immediately when the wetting process was stopped. This phenomenon appeared faster in sensor02s at around 6:10pm while it appeared later in sensor03s at around 7:21pm. It is because when the wetting process stopped, the water started to infiltrate from upper layer (region around sensor 02s) to the lower layer (region around sensor03s). After completion of the whole wetting process, drying process has been done by using a sump pump. The degree of saturation of during drying process is shown in the following Figure 9.

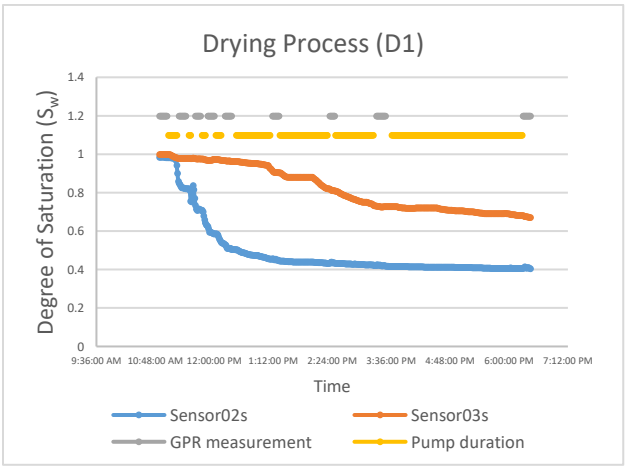

Figure 9 Degree of saturation (S_w) during drying process

From Figure 9, the degree of saturation is higher in region around sensor03s than around sensor02s. It is because the pump was located at the bottom of the soil tank. Water was drawn down from the upper layer (region around sensor02s) to the lower layer (region around sensor03s) when the pump started to pump the water out.

E. GPR data analysis

Besides data from water content sensors, the A-scan of radar signals reflected from 200mm deep metal pipe after several raining processes were discussed in Figure 10. Data are selected after 5th wetting process. Since the reflected hyperbolic signals from 1st to the 4th wetting processes are too obscure. Velocity analysis in these cases is not possible.

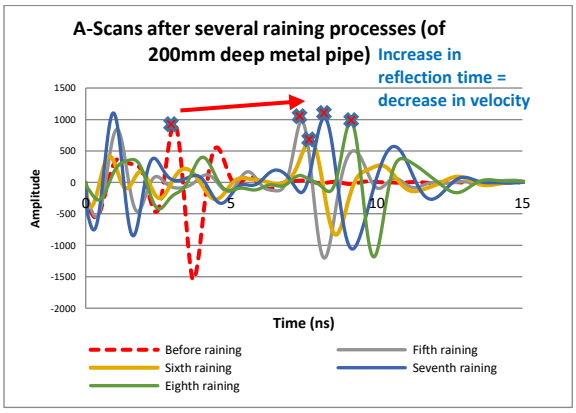

Figure 10 A-scans extracted from the hyperbolic apex of the 200mm deep pipe during the 5th to 8th wetting processes.

As shown in Figure 10, the decrease in velocity of the reflected wave is more significant than the decrease in the reflected signal amplitude as the moisture content of the soil increased. The difference is very obvious between dry condition (before wetting) and wet condition (after fifth wetting). On the other hand, the increasing trend of amplitude and velocity of the wave during the drying process is very obvious. The wave velocity increased gradually with decreasing moisture content (Figure 11). Homogeneity (drying)/heterogeneity (wetting) of water in the soil situation played an important role on this phenomenon.

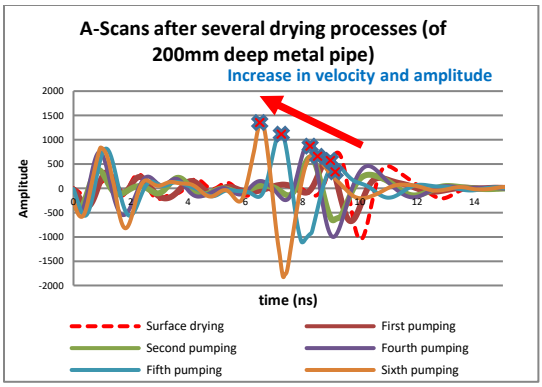

Figure 11 A-scans extracted from the hyperbolic apex of the 200mm deep pipe during the 1st to 6th drying processes.

F. Dielectric hysteresis revealed through RIWD (wetting) and RHWD (drying)

After obtaining the velocities of the GPR signals from the wetting and drying processes, dielectric constant can be derived by Equation (2) and it is correlated with the degree of water saturation in Figure 12 for illustration of dielectric hysteresis during the soil during wet/dry cycle. As mentioned before, data between 1st and 4th wetting process were not valid for velocity analysis since reflected signals from the embedded metal pipe were indistinguishable. Scattering and attenuation during the wetting process cause weakened the reflected hyperbolic signal of the pipes.

Dielectric hysteresis is the dependence of the output of a wetting/drying process, it does not only depend on its current input, but also on its wetting/drying history of past inputs. The dependence arises because the history affects the value of an internal state. Soil dielectric performs hysteresis by continuous wetting and drying cycle of the system. The following Figure 12 shows one of the soil dielectric hysteresis patterns observed from the soil tank sample. The ascending portion of the curve (i.e. wetting), follows a different pathway from the descending portion of the curve (i.e. drying). That means the pattern of dielectric constant depends not only on the degree of water saturation which is a volumetric measure, but also on how water distribute within the bulk soil [14].

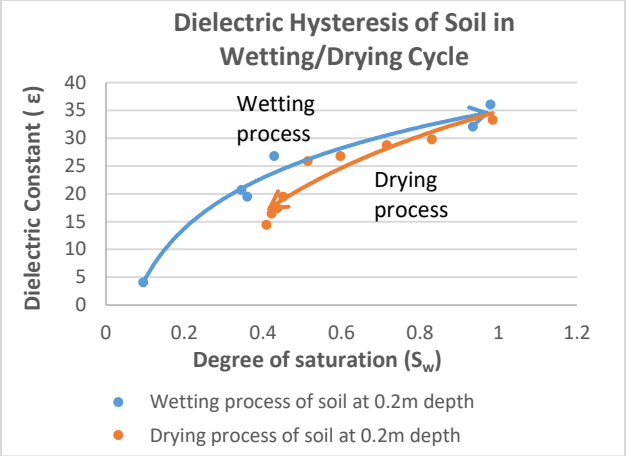

Figure 12 Dielectric hysteresis of soil during wetting/drying cycle

The reason for the above dielectric hysteresis pattern (Figure 12) is because when drying, free water is reduced which causes decrease in both the degree of saturation and dielectric constant. At the same time, some free water turns to bound form which bounded to the soil particles. When the free water turns to bound form during drying process, its magnitude of polarization will be decreased [15]. The decrease in magnitude of polarization is reflected by the decrease in dielectric constant. Hence, the descending portion of the curve (drying) will be lower than the ascending portion of the curve (wetting) at each degree of saturation.

V. Conclusion

It is customary to consider that the volumetric fraction of water in a porous media is the sole important factor affecting dielectric properties of soil, as suggested in various dielectric mixing models. This paper demonstrates another effect, namely RIWD and RHWD, as an often neglected factor on dielectric properties on soil. In this experiment, such factor is realized by experimenting a wetting and drying cycle of plant soil in a tank representing RIWD and RHWD conditions, respectively. The RIWD and RHWD on different dielectric constant were manifested by the phenomenon of dielectric hysteresis. Understanding of this physical phenomenon will lead to future modification of hydrological parameters in dielectric mixing models in NSG applications.

VI. References

[1] F. J. Leij, A. Sciortino, R. Haverkamp, and J. M. S. Ugalde, "Aggregation of vertical flow in the vadose zone with auto- and cross-correlated hydraulic properties," *Journal of Hydrology*, vol. 338, pp. 96-112, May 15 2007.

[2] A. L. Endres, J. P. Jones, and E. A. Bertrand, "Pumping-induced vadose zone drainage and storage in an unconfined aquifer: A comparison of analytical model predictions and field measurements," *Journal of Hydrology*, vol. 335, pp. 207-218, Mar 8 2007.

[3] D. McLaughlin and L. R. Townley, "A reassessment of the groundwater inverse problem," *Water Resources Research*, vol. 32, pp. 1131-1161, May 1996.

[4] J. S. Chen, S. Hubbard, and Y. Rubin, "Estimating the hydraulic conductivity at the South Oyster Site from geophysical tomographic data using Bayesian techniques based on the normal linear regression model," *Water Resources Research*, vol. 37, pp. 1603-1613, Jun 2001.

[5] J. A. Doolittle, B. Jenkinson, D. Hopkins, M. Ulmer, and W. Tuttle, "Hydropedological investigations with ground-penetrating radar (GPR): Estimating water-table depths and local ground-water flow pattern in areas of coarse-textured soils," *Geoderma*, vol. 131, pp. 317-329, Apr 2006.

[6] J. A. Huisman, S. S. Hubbard, J. D. Redman, and A. P. Annan, "Measuring Soil Water Content with Ground Penetrating Radar: A Review," *Vadose Zone Journal*, vol. 2, pp. 476-491, 2003.

[7] J. R. Birchak, C. G. Gardner, J. E. Hipp, and J. M. Victor, "High Dielectric-Constant Microwave Probes for Sensing Soil-Moisture," *Proceedings of the Ieee*, vol. 62, pp. 93-98, 1974.

[8] G. C. Topp, J. L. Davis, and A. P. Annan, "Electromagnetic determination of soil water content: Measurements in coaxial transmission lines," *Water Resources Research*, vol. 16, pp. 574-582, 1980.

[9] W. L. Lai, S. C. Kou, and C. S. Poon, "Unsaturated zone characterization in soil through transient wetting and drying using GPR joint time-frequency analysis and grayscale images," *Journal of Hydrology*, vol. 452-453, pp. 1-13, 2012.

[10] ASTM D6432, "Standard Guide for Using the Surface Ground Penetrating Radar Method for Subsurface Investigation," 2011.

[11] J. F. C. Sham and W. L. Lai, "A New Algorithm for More Accurate Estimation of Wave Propagation Velocity by Common-Offset Survey Method," in *International Symposium Non-Destructive Testing in Civil Engineering (NDT-CE)*, Berlin, Germany, 2015.

[12] K. Roth, R. Schulin, H. Fluhler, and W. Attinger, "Calibration of Time Domain Reflectometry for

Water-Content Measurement Using a Composite Dielectric Approach," *Water Resources Research,* vol. 26, pp. 2267-2273, Oct 1990.

[13] J. F. C. Sham and W. W. L. Lai, "Development of a New Algorithm for Accurate Estimation of GPR's Wave Propagation Velocity by Common-Offset Survey Method," *NDT & E International,* 2016 (Paper submitted).

[14] W. L. Lai, W. F. Tsang, H. Fang, and D. Xiao, "Experimental determination of bulk dielectric properties and porosity of porous asphalt and soils using GPR and a cyclic moisture variation technique," *Geophysics,* vol. 71, pp. K93-K102, 2006.

[15] W. L. Lai, S. C. Kou, W. F. Tsang, and C. S. Poon, "Characterization of concrete properties from dielectric properties using ground penetrating radar," *Cement and Concrete Research,* vol. 39, pp. 687-695, 2009.